DYNAMIC LOAD OF THE LOCOMOTIVE DRIVE CAUSED BY SHORT-CIRCUIT MOTOR TORQUE

Vladimír Zeman*, Zdeněk Hlaváč*

The paper deals with mathematical modelling of dynamic response of the electric locomotive wheelset drive caused by short-circuit traction motor torque. The individual wheelset drive is composed of five subsystems – rotor of the traction motor with driving gear, driven gear, stator of the traction motor with gear housing, hollow graduated shaft with clutches and wheelset. The couplings between subsystems are linearized in dependence on longitudinal creepage and locomotive forward velocity before sudden short-circuit in the asynchronous traction motor. In comparison with previous models of the wheelset drives, the rotor of the electromotor is characterized by flexible shaft supported on flexible rolling-element bearings. The sheet metal packet of cylindrical shape is connected by parallel cooper bars with two short circuit rings. In consequence of strong excitation an interruption of gear mesh can be observed. This nonlinear effect and dynamic load of individual wheelset drive with large number of DOF is investigated using the condensed mathematical model created by modal synthesis method.

Keywords: *electric locomotive, short-circuit torque, condensed model, dynamic load*

1. Introduction

The sudden short-circuit in asynchronous traction motors represents an extreme dynamic loading of wheelset drives of electric locomotives. The short-circuit motor torque in the air-space of the traction motor applied in the electric locomotive developed for speed about 200 km/h by the company ŠKODA TRANSPORTATION was calculated in the production plant ŠKODA ELECTRIC in dependence on time [3]. This torque affects the rotor and conversely the stator for short time period (c. 0.1–0.2 s) and contains the high-frequency harmonic components. On this account a dynamic response of the wheelset drive can not be investigated using torsional models with rigid rotor of the traction motor, as it was shown e.g. in [8], [9]. Only spatial models of the flexible rotor of the traction motor [6] and other components of the wheelset drive [12] enable to investigate the dynamic load. The dynamic response of the wheelset drive caused by short-circuit torque was originally investigated by authors of this article [13] on condition of the rigid rotor supported on rigid bearings and uninterrupted contact in gear mesh between pinion gear mounted on the end of the motor shaft and the gearbox wheel. The bogie frame vibration turned out to be very small. That is why we will suppose that the bogie frame (BF) does not vibrate.

The goal of the paper is to modify the mathematical model of the wheelset drive presented in [13] and use it for dynamic response investigation of the railway vehicle individual wheelset drive caused by short-circuit motor torque.

* prof. Ing. V. Zeman, DrSc., doc. RNDr. Z. Hlaváč, CSc., University of West Bohemia, Faculty of Applied Sciences, Univerzitní 8, 306 14 Plzeň

2. Extended model of the wheelset drive

The new extended mathematical model of the individual wheelset drive is based on computational (physical) model, which structure is shown in Fig.1.

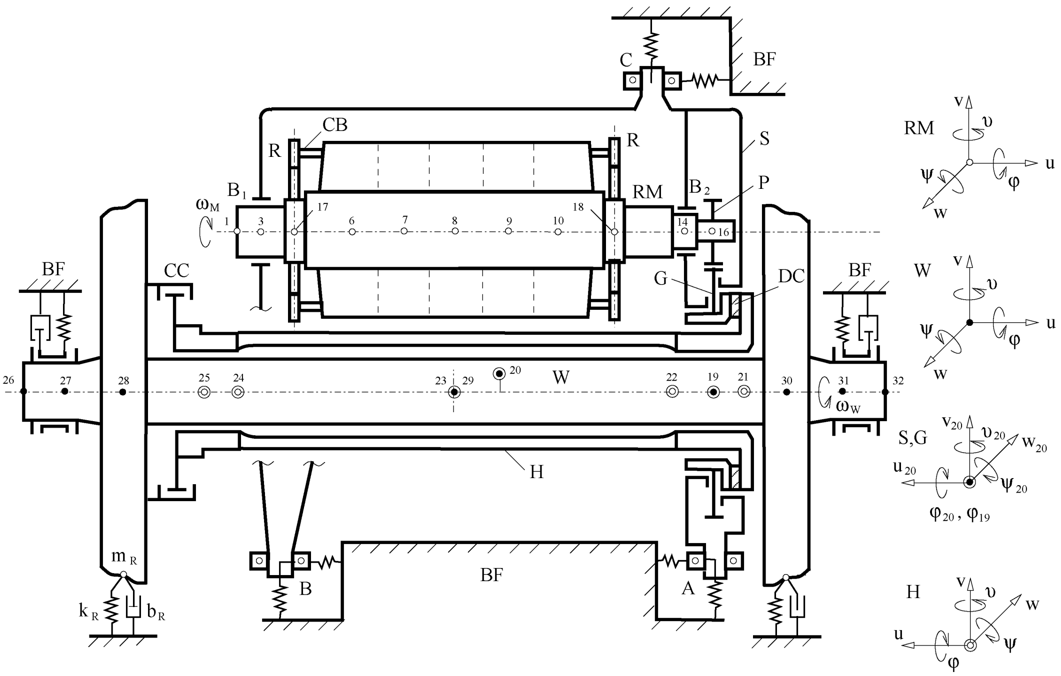

Fig.1: Scheme of individual wheelset drive and coordinate systems

The wheelset drive was decomposed to 5 subsystems:

- *rotor* of traction motor (RM) with pinion gear (P),
- *gearbox wheel* (G) with wheel hub lug and driving part of disc clutch (DC),
- *stator* of traction motor (S) fixed with gearbox,
- *hollow shaft* (H) embrasing the wheelset axle with driven part of disc clutch and driving part of claw clutch (CC),
- *wheelset* (W) with driven part of claw clutch, axle bearings and flexible linkage with track.

The *rotor* model of the traction motor, newly integrated in the drive model, is characterized by a flexible shaft with mounted packet of sheet metals that are equipped with parallel copper bars (CB) connected by end short-circuit rings (R). The shaft is modelled as one-dimensional continuum of beam types on the basis of Rayleigh theory and discretized to 15 finite elements (see Fig. 2) with 16 nodes. The sheet metal packet with copper bars passing trough is modelled by five rigid bodies connected by flexible couplings to the shaft nodes 6 to 10.

Two rings with gravity centres 17 and 18 (see Fig. 2) are connected with the copper bars ends in the outer sides of the rotor. Each ring is supposed to be rigid body with 6 degrees of freedom. The pinion gear is fixed with shaft in end nodal point 16. The shaft is supported by two roller flexible bearings. The mathematical model of the rotor, in comparison with

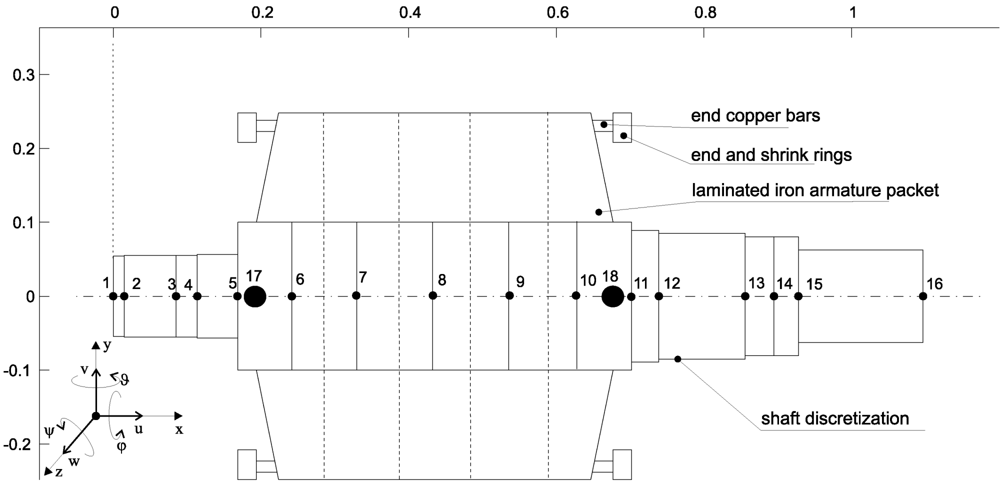

Fig.2: Scheme of rotor model

model in [6], has been completed by the pinion gear in nodal point 16 and is characterized by mass and stiffness matrices $\mathbf{M}_{\mathrm{RM}}$, $\mathbf{K}_{\mathrm{RM}}$ of order 108.

We assume a torsion displacement φ_{19} of the *gearbox wheel* inside the spatially vibrating gearbox, which is fixed with stator of traction motor. Hence, the second subsystem (see Tab. 1) is displayed in the global mass matrix by torsional moment of inertia I_{G} and mass concentrated in centre of gravity is associated with stator.

It is considered that the *stator with gearbox* is a rigid body with centre of gravity in point 20 (see Fig. 1). In configuration space

$$\mathbf{q}_{\mathrm{S}} = [u_{20}, v_{20}, w_{20}, \varphi_{20}, \vartheta_{20}, \psi_{20}] \ , \tag{1}$$

the stator is characterized by mass matrix

$$\mathbf{M}_{\mathrm{S}} = \begin{bmatrix} m_{\mathrm{S}}\,\mathbf{E} & \mathbf{0} \\ \mathbf{0} & \mathbf{I}_{\mathrm{S}} \end{bmatrix} \in R^{6,6} \tag{2}$$

of order 6, where m_{S} is mass, $\mathbf{E}$ unit matrix and $\mathbf{I}_{\mathrm{S}}$ is inertia matrix in coordinate system marked in the Fig. 1 by S with the coordinate basic origin in stator centre of gravity (point 20). The stator with gearbox is connected to the bogie frame by silent blocks with centres of elasticity A, B, C.

The composite *hollow shaft* and the *wheelset* are modelled as spatial vibrating one-dimensional continua discretized by finite element method [11] in nodal points 21–25 (H), 26–32 (W) with rigid disc mounted at nodes 21 (driven part of the disc clutch), 25 (driving part of claw clutch), 27, 31 (journals) and 28, 30 (wheels), respectively.

The viscous-elastic railway balast (rail, railpad, sleeper and balast) is respected by a single mass-spring-damper system [4] defined by mass, stiffness and damping parameters m_{R}, k_{R}, b_{R}. Mathematical models of the hollow shaft and wheelset are characterized by mass and stiffness matrices $\mathbf{M}_{\mathrm{H}}$, $\mathbf{K}_{\mathrm{H}}$ of order 30 and $\mathbf{M}_{\mathrm{W}}$, $\mathbf{K}_{\mathrm{W}}$ of order 42, respectively. Angular speeds of the traction motor ω_{M} and wheelset ω_{W} correspond to pure rolling of the wheelset defined by operational speed v of the electric locomotive.

The vectors of general coordinates $\mathbf{q}_i$ in nodal points i of the one-dimensional continua (shaft of the traction motor, hollow shaft and wheelset) and in the gravity centres of rigid bodies (short circuit rings and stator of the traction motor) have the form

$$\mathbf{q}_i = [u_i, v_i, w_i, \varphi_i, \vartheta_i, \psi_i]^{\mathrm{T}} \ , \quad i = 1{-}18, 20{-}32 \ , \tag{3}$$

where $u_i,\ v_i,\ w_i$ are translational deflections in the corresponding coordinate axes and $\varphi_i,\ \vartheta_i,\ \psi_i$ are rotational deflections around these axes shifted to corresponding node (see Fig. 1). A general position of the subsystems in the local coordinate systems displayed in Fig. 1 is defined by generalized coordinates summarized in Table 1.

Subsystem	Number DOF	Sequence in $\mathbf{q}$	Generalized coordinates
Rotor RM	108	1–108	$u_1, v_1, w_1, \varphi_1, \vartheta_1, \psi_1, \ldots, u_{18}, v_{18}, w_{18}, \varphi_{18}, \vartheta_{18}, \psi_{18}$
Gearbox wheel G	1	109	φ_{19}
Stator S	6	110–115	$u_{20}, v_{20}, w_{20}, \varphi_{20}, \vartheta_{20}, \psi_{20}$
Hollow shaft H	30	116–145	$u_{21}, v_{21}, w_{21}, \varphi_{21}, \vartheta_{21}, \psi_{21}, \ldots, u_{25}, v_{25}, w_{25}, \varphi_{25}, \vartheta_{25}, \psi_{25}$
Wheelset W	42	146–187	$u_{26}, v_{26}, w_{26}, \varphi_{26}, \vartheta_{26}, \psi_{26}, \ldots, u_{32}, v_{32}, w_{32}, \varphi_{32}, \vartheta_{32}, \psi_{32}$

Tab.1: Generalized coordinates of subsystems

The matrices of the mutually isolated subsystems are included in the global matrices of the individual wheelset drive in the form of the block-diagonal structures

$$\mathbf{M} = \mathrm{diag}[\mathbf{M}_{\mathrm{RM}}, I_{\mathrm{G}}, \mathbf{M}_{\mathrm{S}}, \mathbf{M}_{\mathrm{H}}, \mathbf{M}_{\mathrm{W}}] \ , \quad \mathbf{K} = \mathrm{diag}[\mathbf{K}_{\mathrm{RM}}, 0, \mathbf{0}, \mathbf{K}_{\mathrm{H}}, \mathbf{K}_{\mathrm{W}}] \tag{4}$$

accordant with the global vector of generalized coordinates

$$\mathbf{q} = [\mathbf{q}_{\mathrm{RM}}, \varphi_{19}, \mathbf{q}_{\mathrm{S}}, \mathbf{q}_{\mathrm{H}}, \mathbf{q}_{\mathrm{W}}]^{\mathrm{T}} \in R^{187} \ . \tag{5}$$

3. Stiffness matrices of couplings between subsystems

Coupling stiffness matrices between subsystems are derived in configuration space defined in (5). In comparison with previous models in [12], [13], the couplings between rotor and stator of the traction motor and between pinion gear and gearbox wheel are now totally changed. Hence, we will introduce theirs derivation.

The shaft of the rotor is supported on two roller bearings B_1 and B_2, where the left one is the radial-axial (Fig. 3). Principal directions $\eta_i,\ \zeta_i$ of radial bearing stiffnesses $k_{\eta_i},\ k_{\zeta_i}$ include angle α_i with corresponding frame axes $y_i,\ z_i$ ($i = 3, 14$).

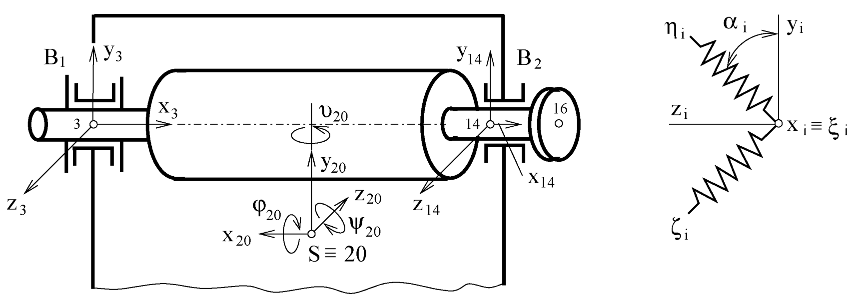

Fig.3: Scheme of the couplings between rotor and stator of the traction motor

The deformation energy of the bearings is given by following form

$$E_{\mathrm{B}} = \frac{1}{2}\,\mathbf{d}_3^{\mathrm{T}}\,\mathbf{K}_3\,\mathbf{d}_3 + \frac{1}{2}\,\mathbf{d}_{14}^{\mathrm{T}}\,\mathbf{K}_{14}\,\mathbf{d}_{14}\ , \tag{6}$$

where $\mathbf{K}_i = \mathrm{diag}[k_{\xi_i}, k_{\eta_i}, k_{\zeta_i}]$, $i = 3, 14$ are diagonal bearing stiffness matrices, whereas $k_{\xi_{14}} = 0$. The transver of the bearing centres caused by stator vibration in the coordinate system of the rotor is described by the vector $\mathbf{T}_{\mathrm{S,RM}}(\mathbf{u}_{20} + \mathbf{R}_i^{\mathrm{T}}\,\boldsymbol{\varphi}_{20})$, where

$$\mathbf{T}_{\mathrm{S,RM}} = \begin{bmatrix} -1 & 0 & 0 \\ 0 & 1 & 0 \\ 0 & 0 & -1 \end{bmatrix}$$

and components of the vector $\mathbf{u}_{20} = [u_{20}, v_{20}, w_{20}]^{\mathrm{T}}$ represent displacements of bearing centres (centre gravity of stator) and the vector $\boldsymbol{\varphi}_{20} = [\varphi_{20}, \vartheta_{20}, \psi_{20}]^{\mathrm{T}}$ describes angle displacements of the stator. Operators $\mathbf{R}_i$ of cross product are defined by radius vectors of bearing centres in coordinate system x_{20}, y_{20}, z_{20}. Deformation vectors of the bearings in coordinate systems ξ_i, η_i, ζ_i of the main stiffness directions of the bearings can be expressed as

$$\mathbf{d}_i = \mathbf{T}_i\,[\mathbf{u}_i - \mathbf{T}_{\mathrm{S,RM}}\,(\mathbf{u}_{20} + \mathbf{R}_i^{\mathrm{T}}\,\varphi_{20})]\ , \quad i = 3, 14\ , \tag{7}$$

where

$$\mathbf{T}_i = \begin{bmatrix} 1 & 0 & 0 \\ 0 & \cos\alpha_i & \sin\alpha_i \\ 0 & -\sin\alpha_i & \cos\alpha_i \end{bmatrix}\ , \quad i = 3, 14 \tag{8}$$

are transformation matrices between vectors in coordinate systems ξ_i, η_i, ζ_i and x_i, y_i, z_i, $i = 3, 14$ and $\mathbf{u}_i = [u_i, v_i, w_i]^{\mathrm{T}}$. The stiffness matrix results from the identity

$$\frac{\partial E_{\mathrm{B}}}{\partial \mathbf{q}} = \mathbf{K}_{\mathrm{RM,S}}\,\mathbf{q}$$

and in the compressed form is

$$\overline{\mathbf{K}}_{\mathrm{RM,S}} = \begin{bmatrix} \mathbf{T}_3^{\mathrm{T}}\,\mathbf{K}_3\,\mathbf{T}_3 & \mathbf{0} & -\mathbf{T}_3^{\mathrm{T}}\,\mathbf{K}_3\,\mathbf{T}_{3,20} \\ \mathbf{0} & \mathbf{T}_{14}^{\mathrm{T}}\,\mathbf{K}_{14}\,\mathbf{T}_{14} & -\mathbf{T}_{14}^{\mathrm{T}}\,\mathbf{K}_{14}\,\mathbf{T}_{14,20} \\ -\mathbf{T}_{3,20}^{\mathrm{T}}\,\mathbf{K}_3\,\mathbf{T}_3 & -\mathbf{T}_{14,20}^{\mathrm{T}}\,\mathbf{K}_{14}\,\mathbf{T}_{14} & \mathbf{T}_{3,20}^{\mathrm{T}}\,\mathbf{K}_3\,\mathbf{T}_{3,20} + \mathbf{T}_{14,20}^{\mathrm{T}}\mathbf{K}_{14}\mathbf{T}_{14,20} \end{bmatrix}\ , \tag{9}$$

where

$$\mathbf{T}_{i,20} = \mathbf{T}_i\,\mathbf{T}_{\mathrm{S,RM}}\,[\mathbf{E}_3, \mathbf{R}_i^{\mathrm{T}}] \in R^{3,6}\ , \quad i = 3, 14\ . \tag{10}$$

The block matrices in (9) are localized in the full stiffness matrix $\mathbf{K}_{\mathrm{RM,S}} \in R^{187,187}$ in accordance with subvectors $\mathbf{u}_3$, $\mathbf{u}_{14}$ and $\mathbf{q}_{20}$ in the global vector $\mathbf{q}$ of generalized coordinates.

The general configuration of spur helical gears (Fig. 4) is described by pinion gear and gearbox wheel vectors of displacements $\mathbf{q}_i$ $(i = 16, 19)$ defined in (3).

In the coordinate system ξ, η, ζ, the vector of relative deviation of the central interaction gearing point can be expressed in the form

$$(\mathbf{d})_{\xi,\eta,\zeta} = \begin{bmatrix} (v_{16} - v_{19})\,\cos\gamma + (w_{16} + w_{19})\,\sin\gamma - r_{\mathrm{P}}\,\varphi_{16} + r_{\mathrm{G}}\,\varphi_{19} \\ -(v_{16} - v_{19})\,\sin\gamma + (w_{16} + w_{19})\,\cos\gamma \\ u_{16} + u_{19} + r_{\mathrm{P}}\,\cos\gamma\,\vartheta_{16} + r_{\mathrm{G}}\,\cos\gamma\,\vartheta_{19} + r_{\mathrm{P}}\,\sin\gamma\,\psi_{16} - r_{\mathrm{G}}\,\sin\gamma\,\psi_{19} \end{bmatrix}\ , \tag{11}$$

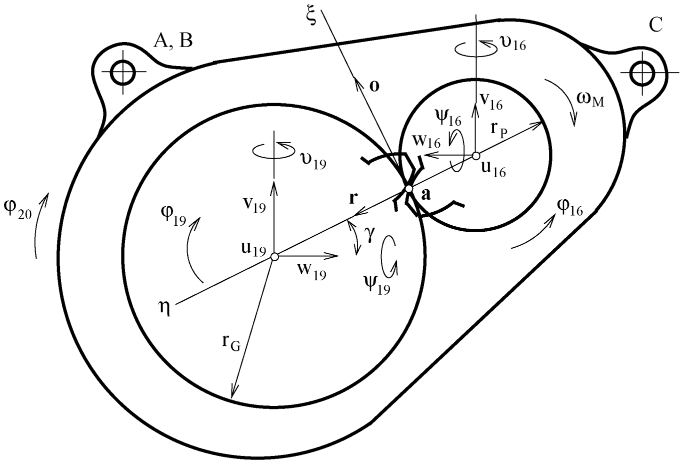

Fig.4: Scheme of a gearing coupling

where $r_{\rm P}$ is rolling radius of the driving pinion gear (driven gearbox wheel $r_{\rm G}$) and γ is angle of position. The gearing deformation is given by vector $(\mathbf{d})_{\xi,\eta,\zeta}$ projection to normal line of the tooth faces

$$d_{\rm n} = \mathbf{e}_n^{\rm T}\,(\mathbf{d})_{\xi,\eta,\zeta} = [\cos\alpha\,\cos\beta, \sin\alpha, \cos\alpha\,\sin\beta]\,(\mathbf{d})_{\xi,\eta,\zeta}\ , \tag{12}$$

where α is normal pressure angle and β is angle of inclination of the teeth. In accordance with (11) and (12) the gearing deformation is

$$d_{\rm n} = \boldsymbol{\delta}_{16}^{\rm T}\,\mathbf{q}_{16} + \boldsymbol{\delta}_{19}^{\rm T}\,\mathbf{q}_{19}\ , \tag{13}$$

where vectors of geometrical parameters of the gear pair are expressed as

$$\boldsymbol{\delta}_{16} = \begin{bmatrix} \cos\alpha\,\sin\beta \\ \cos\alpha\,\cos\beta\,\cos\gamma - \sin\alpha\,\sin\gamma \\ \cos\alpha\,\cos\beta\,\sin\gamma + \sin\alpha\,\cos\gamma \\ -r_{\rm P}\,\cos\alpha\,\cos\beta \\ r_{\rm P}\,\cos\alpha\,\sin\beta\,\cos\gamma \\ r_{\rm P}\,\cos\alpha\,\sin\beta\,\sin\gamma \end{bmatrix}, \quad \boldsymbol{\delta}_{19} = \begin{bmatrix} \cos\alpha\,\sin\beta \\ -\cos\alpha\,\cos\beta\,\cos\gamma + \sin\alpha\,\sin\gamma \\ \cos\alpha\,\cos\beta\,\sin\gamma + \sin\alpha\,\cos\gamma \\ r_{\rm G}\,\cos\alpha\,\cos\beta \\ r_{\rm G}\,\cos\alpha\,\sin\beta\,\cos\gamma \\ -r_{\rm G}\,\cos\alpha\,\sin\beta\,\sin\gamma \end{bmatrix}. \tag{14}$$

The displacement vector $\mathbf{q}_{19}$ of the gearbox wheel can be expressed by its torsional angular displacement φ_{19} and gearbox displacements as

$$\mathbf{q}_{19} = \mathbf{T}_{19,20}\,\mathbf{q}_{20} + [0,0,0,\varphi_{19},0,0]^{\rm T}\ , \tag{15}$$

where transformation matrix

$$\mathbf{T}_{19,20} = \begin{bmatrix} 1 & 0 & 0 & 0 & z_k & -y_k \\ 0 & 1 & 0 & -z_k & 0 & x_k \\ 0 & 0 & 1 & y_k & -x_k & 0 \\ 0 & 0 & 0 & 0 & 0 & 0 \\ 0 & 0 & 0 & 0 & 1 & 0 \\ 0 & 0 & 0 & 0 & 0 & 1 \end{bmatrix}$$

is defined by coordinates x_k, y_k, z_k of the nodal point 19 in the space x_{20}, y_{20}, z_{20}. According to (13) and (15) the gearing deformation is

$$d_\mathrm{n} = \boldsymbol{\delta}_{16}^\mathrm{T}\,\mathbf{q}_{16} + \boldsymbol{\delta}_{19}^\mathrm{T}\,\mathbf{T}_{19,20}\,\mathbf{q}_{20} + r_\mathrm{G}\,\cos\alpha\,\cos\beta\,\varphi_{19}\ . \tag{16}$$

Under the condition of uninterrupted gear mesh and main stiffness k_G of gearing in normal direction, the stiffness gear coupling matrix results from identity

$$\frac{\partial E_\mathrm{d}}{\partial \mathbf{q}} = \mathbf{K}_{\mathrm{P,G}}\,\mathbf{q}\ ,$$

where $E_\mathrm{d} = \frac{1}{2}\,k_\mathrm{G}\,d_\mathrm{n}^2$ is deformation energy of the gear coupling. This matrix in the compressed form is

$$\overline{\mathbf{K}}_{\mathrm{P,G}} = k_\mathrm{G} \begin{bmatrix} \boldsymbol{\delta}_{16}\,\boldsymbol{\delta}_{16}^\mathrm{T} & R_\mathrm{G}\,\boldsymbol{\delta}_{16} & \boldsymbol{\delta}_{16}\,\boldsymbol{\delta}_{19}^\mathrm{T}\,\mathbf{T}_{19,20} \\ R_\mathrm{G}\,\boldsymbol{\delta}_{16}^\mathrm{T} & R_\mathrm{G}^2 & R_\mathrm{G}\,\boldsymbol{\delta}_{19}^\mathrm{T}\,\mathbf{T}_{19,20} \\ \mathbf{T}_{19,20}^\mathrm{T}\,\boldsymbol{\delta}_{19}\,\boldsymbol{\delta}_{16}^\mathrm{T} & R_\mathrm{G}\,\mathbf{T}_{19,20}^\mathrm{T}\,\boldsymbol{\delta}_{19} & \mathbf{T}_{19,20}^\mathrm{T}\,\boldsymbol{\delta}_{19}\,\boldsymbol{\delta}_{19}^\mathrm{T}\,\mathbf{T}_{19,20} \end{bmatrix}\ , \tag{17}$$

where $R_\mathrm{G} = r_\mathrm{G}\,\cos\alpha\,\sin\beta$. The block matrices in (17) are localized in the full stiffness matrix $\mathbf{K}_{\mathrm{P,G}} \in R^{187,187}$ in accordance with subvector $\mathbf{q}_{16}$, angular displacement φ_{19} and subvector $\mathbf{q}_{20}$ in the global vector $\mathbf{q}$ of generalized coordinates.

4. Mathematical model of the individual wheelset drive

To analyze the dynamic response of the wheelset drive caused by the sudden short-circuit traction motor torque, we neglect track and wheel irregularities which are source of kinematic excitation [7]. Let us suppose an operational state of the locomotive running on the straight track before short-circuit which is given by the longitudinal creepage s_0 of both wheels, by forward velocity v [m/s] and by vertical wheel forces N_0 [N].

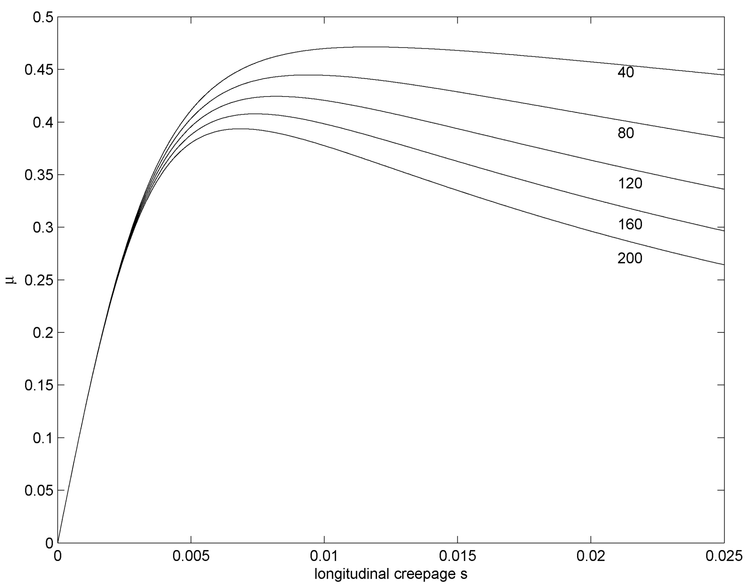

Fig.5: Creep characteristics

Longitudinal $T_{i\,ad}$, lateral $A_{i\,ad}$ creep forces and spin torque $M_{i\,ad}$ acting at the contact patches between rails and wheels can be expressed as [12]

$$T_{i\,\mathrm{ad}} = \mu(s_i, v)\, N_i\ , \quad A_{i\,\mathrm{ad}} = b_{22}\,(\dot{u}_i + r\,\dot{\psi}_i) + b_{23}\,\dot{\vartheta}_i\ , \quad M_{i\,\mathrm{ad}} = -b_{23}\,(\dot{u}_i + r\,\dot{\psi}_i) + b_{33}\,\dot{\vartheta}_i\ . \tag{18}$$

The longitudinal creep coefficient $\mu(s_i, v)$ depends on longitudinal creepage defined by

$$s_i = s_0 + \frac{r\,\dot{\varphi}_i - \dot{w}_i}{v}\ ; \quad s_0 = \frac{r\,\omega_{\mathrm{W}} - v}{v}\ , \tag{19}$$

where r is wheel radius. The lateral creep force and the spin torque about vertical axis depend on linearized creep coefficients b_{ij}, calculated using Kalker's theory [5] for static vertical wheel force before short-circuit. The creep force vectors in coordinate system x_i, y_i, z_i of corresponding wheel can be expressed in the form

$$\mathbf{f}_i^{\mathrm{T}} = [-A_{i\,\mathrm{ad}}, N_i, T_{i\,\mathrm{ad}}, -T_{i\,\mathrm{ad}}\, r, -M_{i\,\mathrm{ad}}, -A_{i\,\mathrm{ad}}\, r]\ , \quad i = 28, 30\ . \tag{20}$$

To analyze the wheelset drive vibration the longitudinal creep characteristics are presented in Fig. 5. These characteristics express longitudinal creep coefficient depending up longitudinal creepage between the wheel and rail and the forward locomotive velocity v [km/h] ($v = 40, 80, 120, 160, 200$). The characteristics in Fig. 5 are calculated for standard adhesion conditions and maximal normal pressure in wheel-rail contact ellipse according to Hertz's theory on the basis of experimentally derived formula presented in [2], [10]. The longitudinal creep coefficient will be linearized in the neighbourhood of a state before short-circuit in the form

$$\mu(s_i, v) = \mu(s_0, v) + \left[\frac{\partial \mu}{\partial s_i}\right]_{s_i = s_0} (s - s_0)\ . \tag{21}$$

The linearized longitudinal creep forces can be then expressed as

$$T_{i\,\mathrm{ad}} = \mu(s_0, v)\, N_0 + b_{11}\,(r\,\dot{\varphi}_i - \dot{w}_i)\ ; \quad b_{11} = \frac{3.6}{v}\, N_0 \left[\frac{\partial \mu}{\partial s_i}\right]_{s_i = s_0}\ . \tag{22}$$

According to (20) and (22) the linearized creep force vectors is

$$\mathbf{f}_i = -\overline{\mathbf{B}}_{\mathrm{ad}}\,\dot{\mathbf{q}}_i + \overline{\mathbf{f}}_0\ , \tag{23}$$

where matrix $\overline{\mathbf{B}}_{\mathrm{ad}}$ and the static force vector $\overline{\mathbf{f}}_0$ are in the form

$$\overline{\mathbf{B}}_{\mathrm{ad}} = \begin{bmatrix} b_{22} & 0 & 0 & 0 & b_{23} & r\,b_{22} \\ 0 & 0 & 0 & 0 & 0 & 0 \\ 0 & 0 & b_{11} & -r\,b_{11} & 0 & 0 \\ 0 & 0 & -r\,b_{11} & r^2\,b_{11} & 0 & 0 \\ -b_{23} & 0 & 0 & 0 & b_{33} & -r\,b_{23} \\ r\,b_{22} & 0 & 0 & 0 & r\,b_{23} & r^2\,b_{22} \end{bmatrix}\ ; \quad \overline{\mathbf{f}}_0 = \begin{bmatrix} 0 \\ N_0 \\ \mu_0\,N_0 \\ -\mu_0\,N_0\,r \\ 0 \\ 0 \end{bmatrix}\ . \tag{24}$$

The vector of global linearized creep forces acting on both wheels in the configuration space of generalized coordinates is than

$$\mathbf{f}_{\mathrm{ad}} = -\mathbf{B}_{\mathrm{ad}}(s_0, v)\,\dot{\mathbf{q}} + \mathbf{f}_0\ , \tag{25}$$

where

$$\mathbf{B}_{\mathrm{ad}}(s_0, v) = \mathrm{diag}[\ldots, \overline{\mathbf{B}}_{\mathrm{ad}}, \ldots, \overline{\mathbf{B}}_{\mathrm{ad}}, \ldots]\ ; \quad \mathbf{f}_0 = [\ldots, \overline{\mathbf{f}}_0^{\mathrm{T}}, \ldots, \overline{\mathbf{f}}_0^{\mathrm{T}}, \ldots]^{\mathrm{T}} \tag{26}$$

with blocks $\overline{\mathbf{B}}_{\mathrm{ad}}$ and subvectors $\overline{\mathbf{f}}_0$ localized on positions corresponding to displacement $\mathbf{q}_i$, $i = 28, 30$ in the vector of generalized coordinates $\mathbf{q}(t)$. Other blocks and subvectors in (26) are zero.

According to the wheelset drive decomposition into 5 subsystems, modelling of the internal couplings between subsystems and linearized creep forces in the neighbourhood of the static equilibrium before perturbation, the mathematical model of the wheelset drive can be written as

$$\begin{aligned} &\mathbf{M}\,\ddot{\mathbf{q}} + [\mathbf{B} + \mathbf{B}_{\mathrm{RM,S}} + \mathbf{B}_{\mathrm{P,G}} + \mathbf{B}_{\mathrm{S,BF}} + \mathbf{B}_{\mathrm{DS}} + \mathbf{B}_{\mathrm{CC}} + \mathbf{B}_{\mathrm{ad}}(s_0, v)]\,\dot{\mathbf{q}} + \\ &\quad + [\mathbf{K} + \mathbf{K}_{\mathrm{RM,S}} + \mathbf{K}_{\mathrm{P,G}}(d_{\mathrm{n}}) + \mathbf{K}_{\mathrm{S,BF}} + \mathbf{K}_{\mathrm{DS}} + \mathbf{K}_{\mathrm{CC}}]\,\mathbf{q} = \mathbf{f}_{\mathrm{M}}(t) + \mathbf{f}_0\ . \end{aligned} \tag{27}$$

Individual damping and stiffness matrices with subscripts correspond to coupling between subsystems (see Fig. 1):

- RM,S – rotor, stator of the traction motor,
- P,G – pinion gear, gearbox wheel,
- S,BF – stator, bogie frame,
- DS – disc clutch between gearbox wheel and hollow shaft,
- CC – claw clutch between hollow shaft and wheelset.

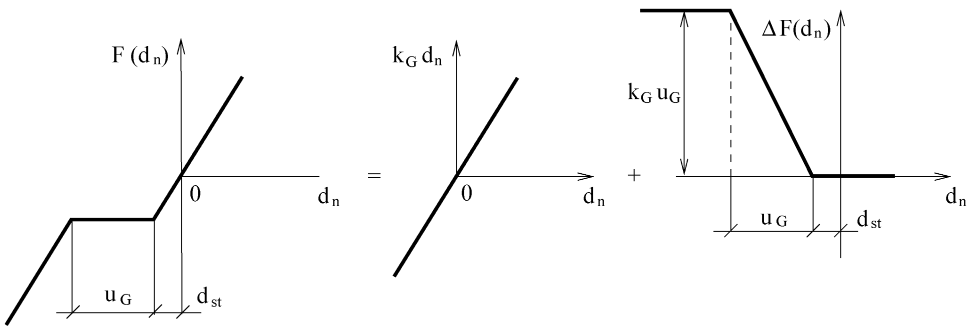

Fig.6: Correction nonlinear stiffness function in gearing

The structure of global damping matrix $\mathbf{B}$ corresponds to stiffness matrix $\mathbf{K}$ in the block diagonal form presented in (4), whereas damping matrices are considered as proportional to corresponding stiffness matrices

$$\mathbf{B}_{\mathrm{RM}} = \beta_{\mathrm{RM}}\,\mathbf{K}_{\mathrm{RM}}\ ;\quad \mathbf{B}_{\mathrm{H}} = \beta_{\mathrm{H}}\,\mathbf{K}_{\mathrm{H}}\ ;\quad \mathbf{B}_{\mathrm{W}} = \beta_{\mathrm{W}}\,\mathbf{K}_{\mathrm{W}}$$

and damping matrices of couplings have the same structure as stiffness coupling matrices. Under the assumption of viscous-elastic gearing including the gear mesh backlash, the resultant force F_{G} transmitted by gearing can be approximately expressed in the following form

$$F(d_{\mathrm{n}}) = k_{\mathrm{G}}\,d_{\mathrm{n}} + \Delta F(d_{\mathrm{n}}) + b_{\mathrm{G}}\,\dot{d}_{\mathrm{n}}\ , \tag{28}$$

where b_{G} approximately expresses viscous damping of oil film between teeth. Mathematically, correction stiffness nonlinear function $\Delta F(d_{\mathrm{n}})$ can be described over three piecewise linear regimes [1] (see Fig. 6)

$$\Delta F(d_{\mathrm{n}}) = \begin{cases} 0 & \text{for} \quad d_{\mathrm{n}} \ge -d_{\mathrm{st}}\ , \\ -k_G(d_{\mathrm{n}} + d_{\mathrm{st}}) & \text{for} \quad -(d_{\mathrm{st}} + u_{\mathrm{G}}) \le d_{\mathrm{n}} \le -d_{\mathrm{st}}\ , \\ k_{\mathrm{G}}\,u_{\mathrm{G}} & \text{for} \quad d_{\mathrm{n}} \le -(d_{\mathrm{st}} + u_{\mathrm{G}})\ , \end{cases} \tag{29}$$

where $u_{\rm G}$ is gear mesh backlash and $d_{\rm st}$ is the static gearing deformation at the time instant of the short-circuit beginning.

The global force vector of gear coupling in general coordinate space (5) can be written as

$$\mathbf{f}_{\rm G}(t,\mathbf{q},\dot{\mathbf{q}}) = \mathbf{K}_{\rm P,G}(d_{\rm n})\,\mathbf{q} + \mathbf{B}_{\rm P,G}\,\dot{\mathbf{q}}\ , \tag{30}$$

where

$$\mathbf{K}_{\rm P,G}(d_{\rm n})\,\mathbf{q} = \mathbf{K}_{\rm P,G}\,\mathbf{q} + \Delta F(d_{\rm n})\,\mathbf{c}_{\rm G} \tag{31}$$

and vector $\mathbf{c}_{\rm G}$ meets the relation $d_{\rm n} = \mathbf{c}_{\rm G}^{\rm T}\,\mathbf{q}$. According to (16)

$$\mathbf{c}_{\rm G} = [\,\dots,\boldsymbol{\delta}_{16}^{\rm T},\dots,r_{\rm G}\,\cos\alpha\,\cos\beta,\boldsymbol{\delta}_{19}^{\rm T}\,\mathbf{T}_{19,20},\dots]^{\rm T}\ . \tag{32}$$

The damping matrix $\mathbf{B}_{\rm P,G}$ of gear coupling has the same structure as stiffness matrix $\mathbf{K}_{\rm P,G}$ defined in (17), only stiffness coefficient $k_{\rm G}$ is replaced by damping coefficient $b_{\rm G}$.

The motor torque during the short-circuit in the air-space of the traction motor is approximated in the form [13]

$$M(t) = M(s_0,v) - M_{\rm C}(t)\ ,\quad M(s_0,v) = 2\,\mu(s_0,v)\,N_0\,r\,\frac{\omega_{\rm W}}{\omega_{\rm M}}\ , \tag{33}$$

where, using Heaviside function $H(t)$, we can write

$$M_{\rm C}(t) = M(s_0,v)\,H(t) + M_0\,{\rm e}^{-D\Omega t}\,\sin[\Omega(t-\Delta t)]\ . \tag{34}$$

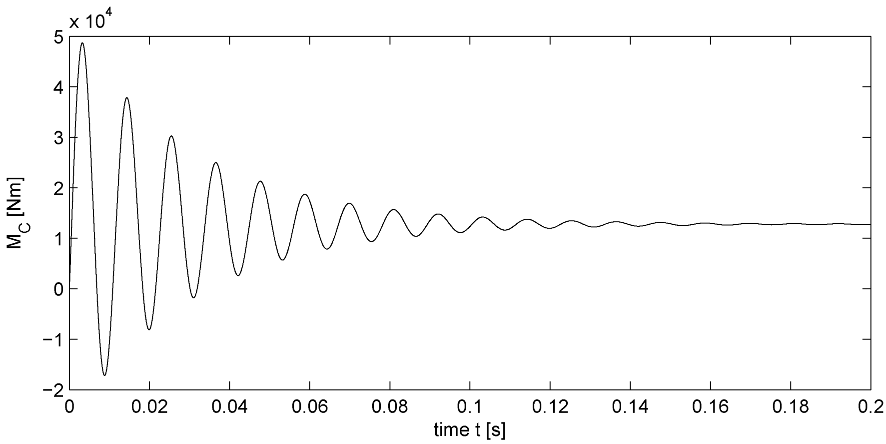

Fig.7: Function approximating the short-circuit torque

The oscillating short-circuit torque $M_{\rm C}(t)$ (Fig. 7) is defined by amplitude M_0, frequency Ω, shift phase $\Omega\,\Delta t$ and torque decay $D\,\Omega$. The total motor torque after short time (here 0.2 [s]) is equal zero ($M_{\rm C} = M(s_0,v)$).

The packet of sheet metals is modelled as a set of five rigid bodies mutually connected with translational, flexural and torsional springs identified on the basis of certain measurement [6]. The motor torque $M(t)$ is described during the short-circuit in mathematical model (27) in the form

$$\mathbf{f}_{\rm M}(t) = \frac{M(t)}{5}\,[\,\dots,1,\dots,1,\dots,1,\dots,1,\dots,1,\dots,5,\dots]^{\rm T} \tag{35}$$

whereas digits 1 are localized on the positions corresponding to torsional displacements of the shaft nodal points 6 to 10 and digit 5 corresponds to stator torsional displacement φ_{20}. Other coordinates symbolized by dots are zero. An opposite sense of the motor torque acting on stator is respected by the stator coordinate system (see Fig. 1).

5. Results of computer simulations

The condensed mathematical model of the wheelset drive with reduced DOF number is used for computer simulations. The DOF number reduction is based on modal transformation of generalized coordinates

$$\mathbf{q}(t) = {}^{m}\mathbf{V}\,\mathbf{x}(t)\ , \tag{36}$$

where ${}^{m}\mathbf{V} \in R^{n,m}$, $m < n$ is modal submatrix of a conservative part of the linearized mathematical model (27)

$$\mathbf{M}\,\ddot{\mathbf{q}}(t) + (\mathbf{K} + \mathbf{K}_{\mathrm{RM,S}} + \mathbf{K}_{\mathrm{P,G}} + \mathbf{K}_{\mathrm{S,BF}} + \mathbf{K}_{\mathrm{DS}} + \mathbf{K}_{\mathrm{CC}})\,\mathbf{q}(t) = \mathbf{0} \tag{37}$$

satisfying the orthonormality conditions ${}^{m}\mathbf{V}^{\mathrm{T}}\,\mathbf{M}\,{}^{m}\mathbf{V} = \mathbf{E}$. The number of chosen master eigenvectors included in modal submatrix is denoted m ($m < n$) and $\mathbf{E}$ is identity matrix of order m. The model (27) in new configuration space of dimension m by using the transformation (36) and relation (31) can be then rewritten in the condensed form

$$\ddot{\mathbf{x}}(t) + {}^{m}\mathbf{V}^{\mathrm{T}}\,\mathbf{B}_{\Sigma}(s_0, v)\,{}^{m}\mathbf{V}\,\dot{\mathbf{x}}(t) + \mathbf{\Lambda}\,\mathbf{x}(t) = {}^{m}\mathbf{V}^{\mathrm{T}}\,[\mathbf{f}_{\mathrm{M}}(t) + \mathbf{f}_0 - \Delta F(d_{\mathrm{n}})\,\mathbf{c}_{\mathrm{G}}]\ , \tag{38}$$

where $\mathbf{B}_{\Sigma}(s_0, v)$ is the shortly marked global damping matrix in the model (27).

The condensed model has to fulfil desired demands on the accuracy. Although this model is nonlinear, we compare the dynamic response of the linearized condensed model (for uninterrupted gear mesh) with the dynamic response of noncondensed model using average relative error

$$\Delta_{m,J} = \frac{1}{n\,J} \sum_{i=1}^{N} \sum_{j=1}^{J} \frac{|q_i(t_j) - q_i^{(m)}(t_j)|}{|q_i(t_j)|}\ , \quad t_j \in \langle 0; T\rangle\ . \tag{39}$$

The influence of the DOF number m and of simulation time interval T [s] is visible in Fig. 8. It is obvious that the condensation level given by $m = 80$ is suitable for a computer simulation.

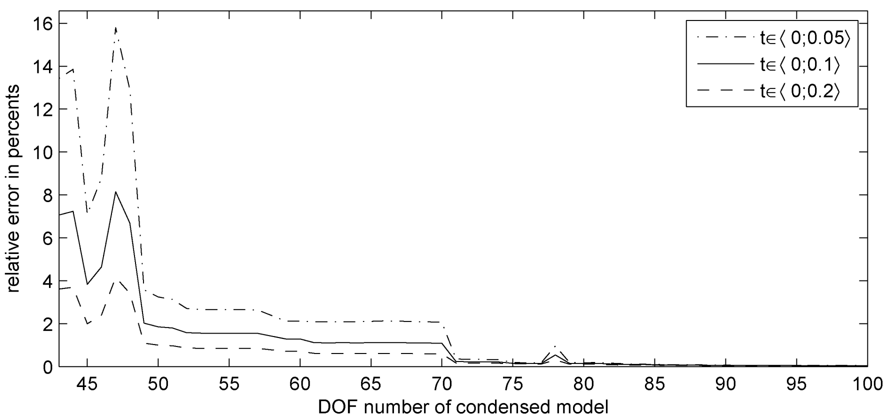

Fig.8: Relative error

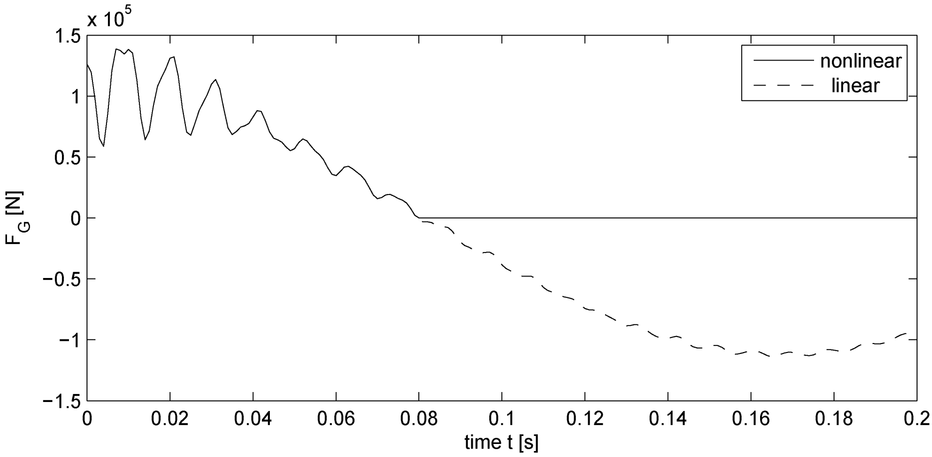

Fig.9: Force transmitted by gearing

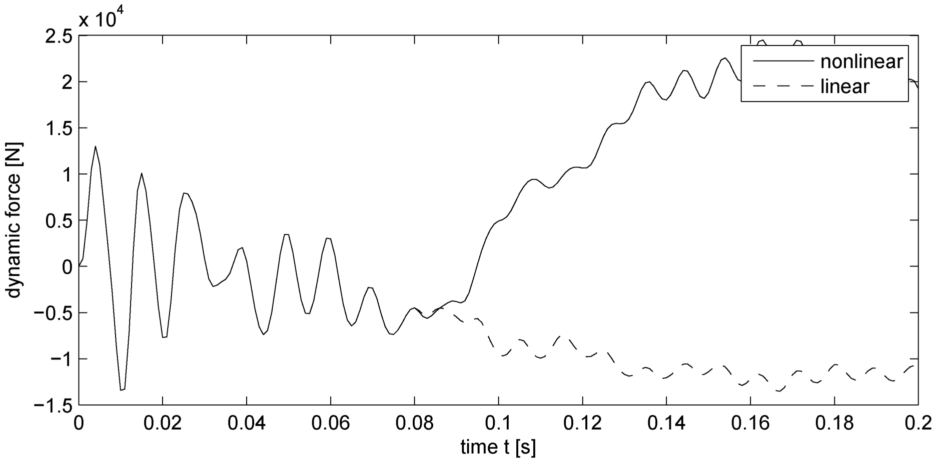

Fig.10: Dynamic force transmitted by silent block B

As an illustration, the time behaviour of chosen values in interval $t \in \langle 0; 0.2\rangle$ [s] for operational parameters $s_0 = 0.005$, $v = 200$ [km/h] and $N_0 = 10^5$ [N] at the instant of the short-circuit are presented in Fig. 9 to Fig. 12. The frequency $f = \Omega/(2\pi) = 90$ [Hz] of the oscilating short-circuit torque and lowest eigenfrequency $f_1 = 2.88$ [Hz], corresponding to couple of complex eigenvalues $-0.0258 \pm \mathrm{i} \cdot 2.88$ [Hz], show up as dominant. At the moment of interrupted gear mesh ($t \doteq 0.08$ [s]) the system becomes nonlinear. The dynamic response of linearized (without of gear backlash) and real nonlinear model with gear backlash are more (e.g. force transmitted by gearing in Fig. 9 and dynamic force transmitted by silent block B in Fig. 10) or less (e.g. dynamic torsion deformation of the coupling between the ring in nodal point 17 and the packet of sheet metals in Fig. 11 and dynamic radial force transmitted by bearing B_2 in Fig. 12) different.

6. Conclusions

The paper describes the new method of mathematical modelling and computer simulation of the individual wheelset drive vibration of the electric locomotive caused by short-circuit

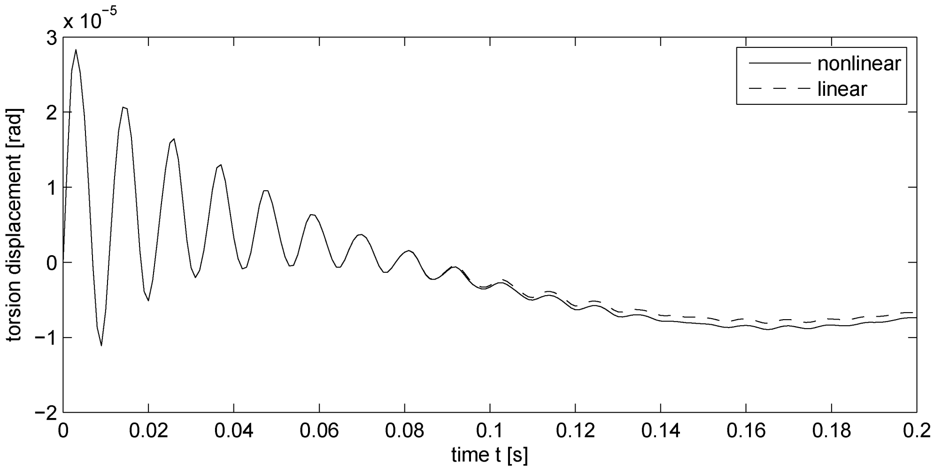

Fig.11: Dynamic torsion deformation of the coupling between ring in nodal point 17 and the packet of sheet metals

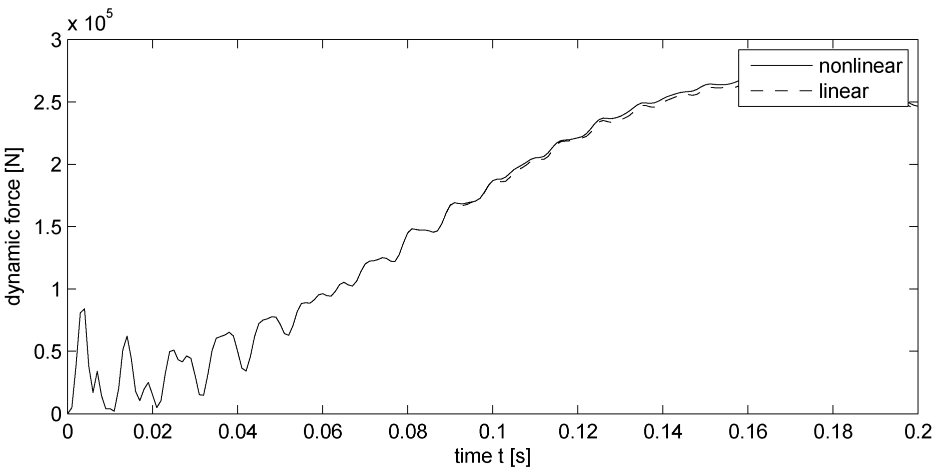

Fig.12: Dynamic component of the radial force transmitted by bearing B_2 (see Fig. 1)

traction motor torque. The torsion, flexure and axial deformations of the motor shaft, flexibility of cooper bars connected sheet metal packet with short-circuit rings and flexibility of the bearings of the rotor are newly respected. The sudden short-circuit in traction motor produces a short-time, but large dynamic load of the wheelset drive components especially in the driving part in front of the disc clutch. In view an extreme short-time internal loading can cause the gear mesh interruption in the gear transmission. This state is dangerous especially for elastic supports of the stator to the bogie frame by silent blocks.

The developed software in MATLAB code enables graphically record the time behaviour of the arbitrary generalized coordinate and the forces transmitted by linkages between wheelset drive components. The dynamic response depends on operational parameters (especially on longitudinal creepage) at the instant just before the short-circuit. Fundamentally worseness arises in the event of the short-circuit at large longitudinal creepage in the downward section of the creep characteristics (see Fig. 5), when the system is unstable. The wheelset drive condensed mathematical model with reduced DOF number is a suitable instrument for computer simulations of the large nonlinear system in the case of interrupted gear mesh.

Acknowledgement

This paper has been elaborated in a framework of the projects MŠMT 1M0519 – Research centre of Rail Vehicles and MSM 4977751303 of the Ministry of Education, Youth and Sports of the Czech Republic.

References

[1] Byrtus M., Zeman V.: On modeling and vibration of gear drives influenced by nonlinear couplings, Mechanism and Machine theory, Vol.46 (2011), No. 3, 375–397

[2] Čáp J.: Some aspects of uniform comment of adhesion mechanism, Proceedings of VŠCHT Pardubice works, 1993, pp. 26–35 (in Czech)

[3] Dvořák P.: Calculated values of the short-circuit moment in the air-space of the traction motor ML 4550 K/6, Documentation of ŠKODA ELECTRIC a.s., Plzeň, 2009 (in Czech)

[4] Feldman V. et all.: Monitoring the dynamic of railway track by means of the Karhunen-Loeve-transfomation, in System Dynamics and Long Term Behaviour of Railway Vehicles, Track and Subgrade (K. Popp and W. Schiehlen eds.), Springer, 2003, pp. 231–246

[5] Garg V., Dukkipati R.: Dynamics of railway vehicle systems, London Academic Press 1984, Toronto

[6] Hajžman M., Byrtus M., Zeman V.: Development of the basic dynamical model of a squirrel cage motor, Engineering Mechanics, Vol. 17 (2010), No. 3/4, 161–172

[7] Hlaváč Z., Zeman V.: Optimization of the railway vehicle bogie in term of dynamic, Applied and Computational Mechanics, 1 (3) (2009), 39–50

[8] Jöckel A.: Aktive Dämpfung von Ratterschwingungen in Antriebstrang von Lokomotive mit Drehstrom-Antriebstechnik, ZEV + DET Glas. Ann., 125 (5) (2001), 191–204

[9] Lata M.: Modelling of transient processes in torsion drive system of railway vehicle, Scientific Papers of the University of Pardubice, Series B, 2003, pp. 45–58 (in Czech)

[10] Lata M.: Dynamic processes in electric locomotive drive on rise of the wheelset slip, Book of Extended Abstracts of the Conference Engineering Mechanics 2004, Svratka, pp. 165–166, (full paper on CD-ROM)

[11] Slavík J., Stejskal V., Zeman V.: Dynamic of machines principles, CTU Publishing House 1997, Praha (in Czech)

[12] Zeman V., Hlaváč Z., Byrtus M.: Modelling of wheelset drive vibration of locomotive 109E, Research report n. H2,H6-06-01/2006, Research Centre of Rail Vehicles, Plzeň, 2007 (in Czech)

[13] Zeman V., Hlaváč Z.: Dynamic wheelset drive load of the railway vehicle caused by short-circuit motor moment, Applied and Computational Mechanics, Vol. 3 (2009), No. 2, 423–434

Received in editor's office: March 17, 2011
Approved for publishing: May 4, 2011

Note: This paper is an extended version of the contribution presented at the national colloquium with international participation *Dynamics of Machines 2011* in Prague.